

THE LONG-PERIOD RADIO TRANSIENT AND CATAclySMIC VARIABLE ASKAP J1745-5051: EVIDENCE FOR A 15,000 K WHITE DWARF AND A SUB-STELLAR DONOR

CHRISTIAN KNIGGE[Ⓢ]

School of Physics and Astronomy, University of Southampton, Highfield, Southampton SO17 1BJ, UK

SIMONE SCARINGI[Ⓢ]†

Centre for Extragalactic Astronomy, Department of Physics, Durham University, South Road, Durham, DH1 3LE and
INAF-Capodimonte Astronomical Observatory, Salita Moiariello 16, 80131 Naples, IT

NOEL CASTRO SEGURA[Ⓢ]†

Department of Physics, University of Warwick, Gibbet Hill Road, Coventry CV4 7AL, UK

DOMITILLA DE MARTINO[Ⓢ]

INAF-Capodimonte Astronomical Observatory, Salita Moiariello 16, 80131 Naples, IT

MARTINA VERESVARSKA[Ⓢ]

Institute of Space Sciences (ICE, CSIC), Campus UAB, Carrer de Can Magrans s/n, E-08193 Barcelona, Spain
Institut d'Estudis Espacials de Catalunya (IEEC), 08860 Castelldefels (Barcelona), Spain

Version June 30, 2026

Abstract

Long-period transients (LPTs) are radio sources that exhibit highly polarized periodic radio bursts on time-scales of minutes to hours. At least some LPTs are associated with white dwarfs (WDs) in close binary systems. However, the evolutionary connection – if any – between LPTs and accreting WDs (aka “cataclysmic variables” [CVs]) has been unclear. Against this background, the recent discovery of ASKAP J174508.9-505149 has been a breakthrough: this system is a bona-fide LPT that is also an X-ray emitting magnetic CV (mCV) with an orbital period of $P_{orb} \simeq 1.3$ hrs. Here, we construct the broad-band far-ultraviolet through near-infrared spectral-energy distribution (SED) for the system and show that this is well described by two components: a $T_{eff} \simeq 15,000$ K WD (which dominates the far-UV through optical bands) and a sub-stellar ($M_2 \simeq 0.05 M_{\odot}$, $T_{eff} \simeq 1800$ K) donor star (which dominates in the K_s band). Our SED-fitting results differ significantly from those in the discovery paper for four reasons: (i) we fix an issue with the treatment of reddening/extinction; (ii) we discard photometric measurements that are irreparably contaminated by an unrelated star located just $0.9''$ from ASKAP J174508.9-505149; (iii) we add near-infrared brightness measurements obtained from PSF-fitting photometry on archival VISTA/VHS observations; (iv) we fit the data with synthetic spectra based on model atmospheres (rather than with blackbodies). The inferred WD temperature is reasonable for an accretion-heated primary in a short-period mCV. The sub-stellar nature of the donor suggests that the system has already evolved past the CV period minimum, i.e. that it is a “period bouncer”. The SED fit also yields a distance of $d \simeq 320$ pc, only $\simeq 4\times$ larger than that to the nearest confirmed mCV. Since the beaming fraction (the fraction of the sky swept out by the radio beam) is likely to be small, systems like ASKAP J174508.9-505149 could actually make up a large percentage of mCVs. This may point towards a connection between LPTs and the long-standing problem of the “missing” population of period bouncers among CVs.

Subject headings: stars: binaries: close, stars: white dwarfs, radio continuum: transients, X-rays: binaries

c.knigge@soton.ac.uk
simone.scaringi@durham.ac.uk
simone.scaringi@durham.ac.uk
noel.castro-segura@warwick.ac.uk
domitilla.demartino@inaf.it
mveresvarska@ice.csic.es

† These authors contributed comparably to this project.

1. INTRODUCTION

Long-Period Transients (LPTs) are radio sources that exhibit highly polarized periodic radio bursts on time-scales of minutes to hours. Since the discovery of the proto-type GLEAM-X J1627-5235 (Hurley-Walker et al. 2024), about a dozen LPTs have been identified (Rea et al. 2026). However, their physical nature remains unclear. Even though polarized radio pulses are commonly seen in pulsars and magnetars, the typical recurrence time-scales in those systems are sub-second. And while the time-scales seen in LPTs are similar to those found in “WD pulsars” (see below), LPTs can be significantly more luminous and polarized than those systems. Despite these challenges, scenarios involving slow-spinning magnetars and highly magnetic WDs are generally favoured. However, much more exotic scenarios have been proposed as well, including models involving primordial black holes, self-lensed pulsar/black-hole binaries, intermediate mass black holes and strange stars (for a review, see Rea et al. 2026).

Models involving magnetic WDs are particularly appealing, since at least some LPTs have been associated with WD binary systems. More specifically, before the discovery of ASKAP J174508.9-505149 (referred to as ASKAP J1745-5051 hereafter), only two LPTs had been firmly established as such on the basis of their spectral energy distribution and radial velocity (RV) variations: GLEAM-X J0704-36 (Hurley-Walker et al. 2024; Rodriguez 2025) and ILT J1101+5521 (de Ruiter et al. 2025). Two additional LPTs are strong WD binary candidates without RV confirmation: ASKAP J1448-6856 (Anumarlapudi et al. 2025) and CHIME J1634+44 (Blout et al. 2025). The optical/infrared counterparts of the remaining LPTs are either unknown or uncertain (e.g. Pelisoli et al. 2025; Rea et al. 2026).

Prior to the recognition that (some) LPTs are associated with WD binaries, two flavours of radio-emitting magnetic WDs in close binary systems were known: one being accreting (the “magnetic cataclysmic variables”, mCVs), the other non-accreting (the “WD pulsars”; Marsh et al. 2016; Pelisoli et al. 2023; Castro Segura et al. 2025). In mCVs, the WD accretes material from a Roche-lobe-filling companion. This material is channelled onto the WD surface along magnetic field lines, either directly from the inner Lagrangian point (the so-called “polars”) or from the inner edge of a truncated accretion disk (the “intermediate polars”; for a review of AWD, see e.g. Warner 1995). In polars, the WD spins synchronously with the orbit, i.e. $P_{spin} = P_{orb}$ (with a few systems known as asynchronous polars out of synchronism by a few percent); in intermediate polars, $P_{spin} < P_{orb}$. Radio emission from mCVs is reviewed by Barrett et al. (2020). In the “WD pulsars” – the proto-type being AR Sco (Marsh et al. 2016) – the donor star does not fill its Roche lobe, so the system is detached (Pelisoli et al. 2022). The radio emission in these systems is thought to be powered by the interaction of the magnetic fields of the WD and its companion (Buckley et al. 2017; Garnavich et al. 2019), however the mechanism behind the pulsing behaviour is still debated (e.g. Geng et al. 2016; Katz 2017; Takata et al. 2018; Potter & Buckley 2018; du Plessis et al. 2022; Barrett & Gurwell 2025). An evolutionary scenario proposed by Schreiber

et al. (2021) links WD pulsars to magnetic CVs, suggesting that accreting WDs may generate stronger magnetic fields as they age and potentially evolve from intermediate polars through a detached WD pulsar phase into polars. However, the high temperatures observed in accreting WDs challenge this picture, as compressional heating may inhibit or delay the emergence of crystallization-driven magnetic fields (Garnavich et al. 2021; Pelisoli et al. 2024; Castro-Tapia et al. 2024; Camisassa et al. 2024). Therefore, the evolutionary state of these systems – and their connection to mCVs – is still poorly understood.

LPTs have been proposed as possible intermediaries between WD pulsars and polars (Rodriguez 2025), but the low temperatures of most of the WDs seen in LPTs – $T_{WD} \simeq 5\text{--}7 \times 10^3 \text{ K}$ – make this connection non-trivial. Such cool temperatures would require the WD pulsar progenitors to have avoided substantial accretion heating and to have entered the pulsar phase already relatively cold. The warmer WDs observed in the closest known WD pulsars, with $T_{WD} \simeq 11500 \text{ K}$, therefore pose a challenge to this picture (Garnavich et al. 2021; Pelisoli et al. 2024). In contrast, Yang (2026) proposed that some LPTs may instead originate from magnetic WD–MD binaries in the pre-mCV phase. There, asynchronous rotation between the WD and the binary orbit can sustain either unipolar-inductor emission or magnetospheric interaction, with the dominant mechanism determined by the relative magnetic moments of the WD and its companion.

Against this background, the recent discovery of ASKAP J1745-5051 as the first LPT that is also clearly an accreting mCV is extremely significant (Rose et al. 2026). Based on the discovery paper and the follow-up X-ray study by Imbrogno et al. (2026), the system is most likely a polar mCV (or possibly one of the rare *slightly* “asynchronous polars”), since all timing signals – from radio, optical and X-ray bands – appear to be consistent with a unique (presumably orbital) period. Yet its radio properties also clearly establish it as a bona-fide LPT. ASKAP J1745-5051 therefore promises to be the “missing link” between LPTs, mCVs and perhaps WD pulsars. The obvious analogy here is with the “transitional millisecond pulsars” (tmSPs), which switch between accretion-powered X-ray-binary (XRB) and rotation-powered radio-pulsar states (Papitto & de Martino 2022). It was the discovery of the proto-typical tmSP PSR J1023+0038 by Archibald et al. (2009) that conclusively established the evolutionary connection between XRBs and MSPs.

Unfortunately, many of the basic observational properties of ASKAP J1745-5051 remain unknown. For example, while the source has a *Gaia* counterpart, its parallax ($\pi = 1.75 \pm 0.91 \text{ mas}$) is essentially unconstrained (*Gaia* Collaboration et al. 2023). Partly as a result of this, the two-blackbody SED fits carried out by Rose et al. (2026) could only place rough constraints on the system component(s) that dominate in the ultraviolet and optical bands.

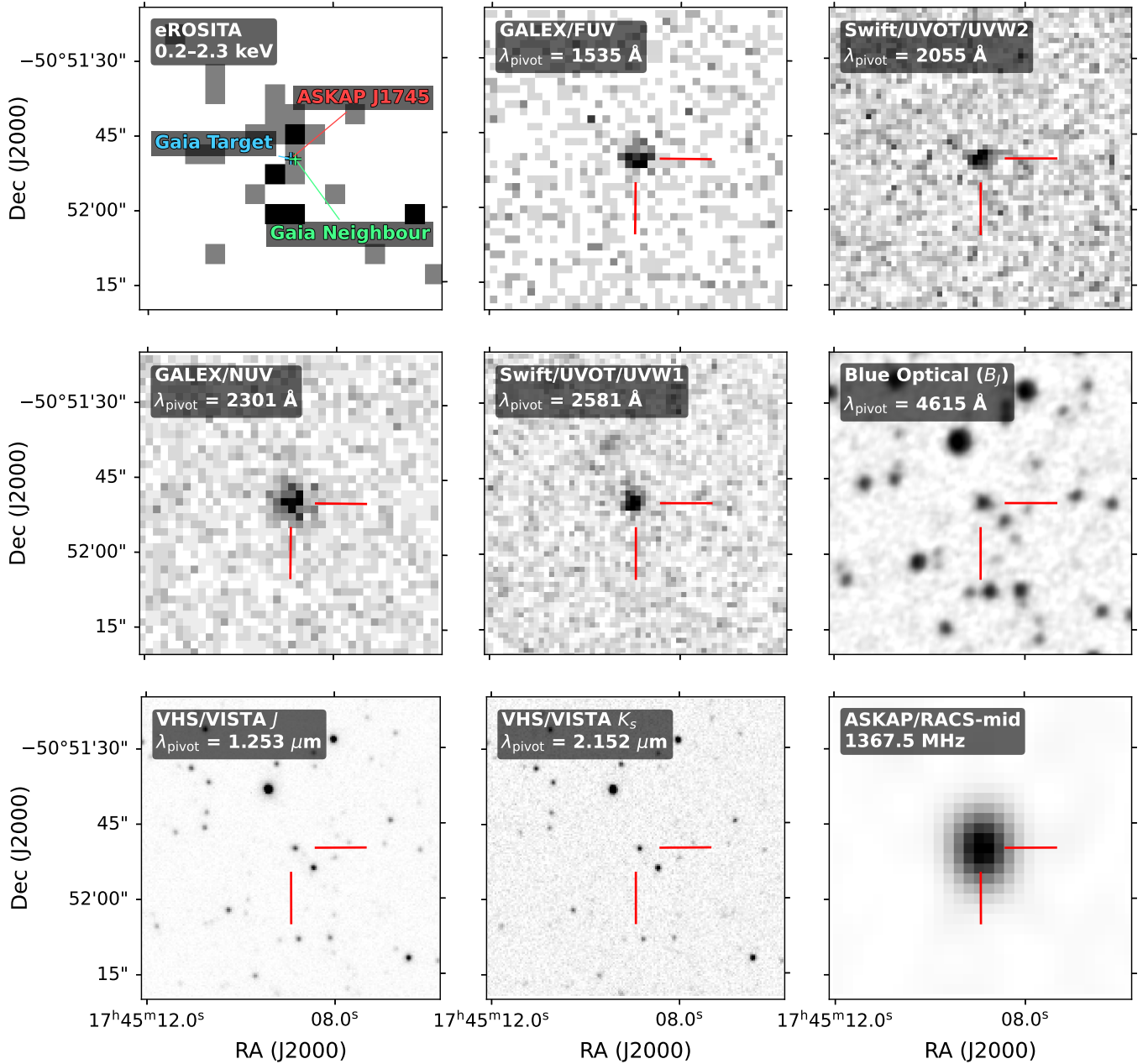


FIG. 1.— $1' \times 1'$ finding charts centered in ASKAP J1745-5051 covering wavelengths from X-ray to radio. In the top left panel the position of the ASKAP J1745-5051 and the two *GAIA* sources are shown with coloured crosses.

The purpose of this paper is to improve on this situation. More specifically, in Section 2 we first construct a wider and more reliable broad-band SED for the system. This involves (i) fixing an issue with the reddening corrections applied by [Rose et al. \(2026\)](#) to the ultraviolet and optical fluxes; (ii) discarding photometric measurements based on optical images in which ASKAP J1745-5051 is irreparably blended with an apparently unrelated close neighbour of comparable optical brightness; and (iii) adding near-infrared measurements obtained via PSF-fitting photometry on VISTA/VHS images. In Section 3, we then fit the resulting SED with a model consisting of two synthetic spectra: a DA WD primary and a low-mass, stellar or sub-stellar secondary. As we shall see, the data is reasonably well described by the combination of a $\simeq 15,000$ K WD and a cool

($T \simeq 1700$ K – 2000 K) sub-stellar ($M_2 \simeq 0.05 M_\odot$) secondary. In Section 4, we discuss the implication of these results for understanding ASKAP J1745-5051, specifically, and the connection between LPTs and mCVs, more generally. Finally, in Section 5, we summarize our conclusions.

2. SED CONSTRUCTION

We used the data sources listed in [Rose et al. \(2026\)](#) as a starting point for constructing our broad-band SED of ASKAP J1745-5051. After searching for additional archival observations of the field, we supplemented the [Rose et al. \(2026\)](#) data set with near-IR observations obtained by the VHS Survey ([McMahon et al. 2013](#)). Table 1 provides a summary of the observations we have used in this work and the corresponding photometric

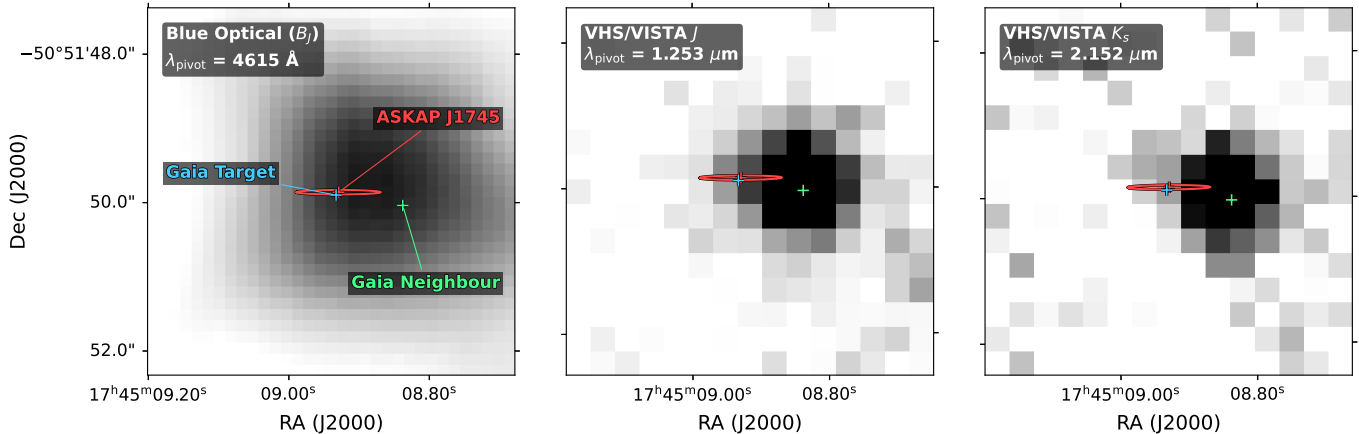


FIG. 2.— $5'' \times 5''$ finding charts from the highest-resolution images centred on ASKAP J1745-5051, showing the positions of the two *Gaia* sources, marked by light yellow and blue crosses, and the position of the LPT ASKAP J1745-5051 derived from radio observations, indicated by the red ellipse centred on the red cross. The images show clearly how the position of the radio source can be uniquely identify with the *Gaia* counterpart, it also illustrate the blending of the two sources, and demonstrate that the interloper dominates the redder bands.

measurements. Finding charts for all wavebands, covering a $1' \times 1'$ field centered on the target, are provided in Figure 1.

We note that Table 1 lists one set of Swift/UVOT observations (in the near-UV UVW2, UVM2 and UVW1 filters), but there are actually two sets in the archive. As discussed by Rose et al. (2026), the first (ID00016563001) was much shorter than the second (ID00016563005). Inspection of the images shows that the first observation also suffered from poor tracking. We therefore only use the second set of observations for the present study.

We do not apply any reddening correction to the observed brightness estimates, choosing instead to deal with extinction as part of our modelling². The photometric data used by Rose et al. (2026) for their SED fitting is provided in their Supplementary Table 1. This is meant to include a correction for reddening by $E(B - V) = 0.2$. However, their extinction-corrected magnitudes are *fainter* than the uncorrected ones. Since they have kindly made their data set and analysis code public, we have been able to trace this to a bug in their extinction-correction routine. The code inadvertently *applies* extinction to the data, rather than *correcting* for it.

2.1. An Interloper Within $1''$ from ASKAP J1745-5051

The *Gaia* DR3 catalogue reveals that ASKAP J1745-5051 (*Gaia* DR3 ID: 5946454415417964032; $m_G = 19.45$) is located just $0.9''$ from a slightly brighter optical source (*Gaia* DR3 ID: 5946454411127231488; $m_G = 19.33$). Figure 2 shows a zoom-in on the central $5'' \times 5''$ region around ASKAP J1745-5051 in our highest resolution (blue optical and near-IR) images. The existence of this neighbour was already noted by Rose et al. (2026). However, its presence means that the *Gaia* B_p and R_p estimates for ASKAP J1745-5051 are unreliable: the effective spatial resolution of *Gaia* is $\simeq 0.1''$ in the G-band, but only $2'' - 3''$ in the B_p and R_p bands (Babusiaux et al. 2023).

The problem can be confirmed quantitatively via *Gaia*'s `phot_bp_rp_excess_factor` parameter, which is

² One of the first author's mottos is "Mess with the model, not the data."

defined as the flux ratio $(F_{B_p} + F_{R_p})/F_G$. For a well-behaved isolated source, this ratio should be $\simeq 1$. Values above $\simeq 1.3$ indicate significant blending problems. For the *Gaia* counterpart to ASKAP J1745-5051, `phot_bp_rp_excess_factor` = 2.89. We therefore caution that the location of ASKAP J1745-5051 in the *Gaia* CMD shown by Rose et al. (2026) is unreliable. We thus do not include the *Gaia* B_p and R_p estimates in our broad-band SED.³

It is worth noting that there are currently *no* optical images of the field in which ASKAP J1745-5051 can be resolved from its neighbour. The MAMA scan of the SERC-J photographic plate shown in Figures 1 and 2 is likely to be the highest resolution image available, and it is clearly not sufficient to attempt deblending via PSF-fitting. The only modern CCD-based optical images of the field come from the SkyMapper survey, but the PSF in these images has FWHM $\simeq 2.5'' - 3.2''$ (Onken et al. 2019). As it stands, the *Gaia* G-band magnitude is the *only* reliable optical brightness measurement for ASKAP J1745-5051.

The neighbouring star appears to be unrelated to ASKAP J1745-5051. Neither source has a meaningful parallax, presumably due to the blending problem (ASKAP J1745-5051: $\pi = 1.75 \pm 0.91$ mas; neighbour: $\pi = 1.03 \pm 0.54$ mas). However, they do have very different proper motions (ASKAP J1745-5051: $\mu_\alpha = 2.98 \pm 0.85$ mas yr⁻¹, $\mu_\delta = 3.77 \pm 0.75$ mas yr⁻¹; neighbour: $\mu_\alpha = -1.72 \pm 0.51$ mas yr⁻¹, $\mu_\delta = 8.43 \pm 0.44$ mas yr⁻¹). These values seem irreconcilable, even if we allow for additional systematic uncertainties associated with blending.

Importantly, despite the presence of the interloper, the association of the radio, X-ray and UV sources with *Gaia* DR3 5946454415417964032 is secure. As shown in Figure 2, the position of the radio source is precise enough to

³ The extent to which the published $B_p - R_p$ colour is offset from the true value depends on how similar the intrinsic colour of ASKAP J1745-5051 is to that of its neighbour. The published colours are $B_p - R_p = 1.08$ (ASKAP J1745-5051) and $B_p - R_p = 1.49$ (neighbour). However, since blending will tend to average out the colour differences, these estimates are bound to be more similar than the true values.

TABLE 1
SUMMARY OF MULTI-WAVELENGTH OBSERVATIONS USED IN THIS WORK.

| Observatory / Instrument / Survey | Band / Filter | Type | Centre | Flux / Magnitude | Units / System | Observation Date | Comments |
|---|------------------|-----------------|---------------------|--------------------------------------|---------------------------|-------------------------|--|
| eROSITA/SRG | 0.2–2.3 keV | X-ray | 1 keV | -12.51 ± 0.08 | $\log(\text{erg/s/cm}^2)$ | 2020-03-26 | Only used in finder chart. |
| GALEX/AIS | FUV | Far-UV | 1535 Å | 19.84 ± 0.15 | AB | 2006-08-09 | ... |
| Swift/UVOT | UVW2 | Near-UV | 2055 Å | 18.47 ± 0.16 | Vega | 2024-05-16 | ... |
| Swift/UVOT | UVM2 | Near-UV | 2231 Å | 18.18 ± 0.15 | Vega | 2024-05-16 | ... |
| GALEX/AIS | NUV | Near-UV | 2301 Å | 19.67 ± 0.11 | AB | 2006-08-09 | ... |
| Swift/UVOT | UVW1 | Near-UV | 2581 Å | 18.96 ± 0.20 | Vega | 2024-05-16 | ... |
| SERC-J/MAMA | B_J | Blue optical | 4615 Å | ... | ... | 1975-08-08 | UKST SERC-J survey plate J 1756 (field 228), digitised by the Observatoire de Paris MAMA scanner. Target blended with neighbour. Only used in finder chart |
| Gaia/DR3 | G | Wide optical | 6218 Å | 19.45 ± 0.04 | Gaia | ... | Observations span 2014-07-25 to 2017-05-28. Gaia→Vega offset $\simeq 0.03$ mag (applied in SED fit). |
| VISTA/VIRCAM/VHS | J | Near-IR | 1.253 μm | 19.19 ± 0.10 19.79 ± 0.16 | Vega | 2014-07-28 | Gaussian-PSF fit Moffat-PSF fit |
| VISTA/VIRCAM/VHS | K_s | Near-IR | 2.152 μm | 18.48 ± 0.18 18.69 ± 0.21 | Vega | 2014-07-28 T03:10:33 | Gaussian-PSF fit Moffat-PSF fit |
| VISTA/VIRCAM/VHS | K_s | Near-IR | 2.152 μm | 18.32 ± 0.16 18.47 ± 0.18 | Vega | 2014-07-28 T03:08:36 | Gaussian-PSF fit Moffat-PSF fit |
| ASKAP/RACS | mid | Radio | 1367.5 MHz | 22.40 ± 0.36 | mJy | 2020-12-27 | Only used in finder chart. |

uniquely identify the correct *Gaia* counterpart. Since the sky densities of radio, X-ray and UV sources are low, the probability that these sources are chance coincidences is negligible. Moreover, [Rose et al. \(2026\)](#) have detected the period seen in the radio data also in optical spectroscopy, and [Imbrogno et al. \(2026\)](#) have detected the same period also in X-rays.

2.2. Estimating The Near-IR Brightness of ASKAP J1745-5051

The VISTA/VHS images have *just* enough spatial resolution – FWHM $\simeq 0.9''$ – to warrant an attempt at PSF-fitting to estimate the near-IR brightness of ASKAP J1745-5051. We have therefore downloaded the relevant images and carried out PSF-fitting photometry as follows. For each image, we run a source detection algorithm on a $1'$ radius field centered on ASKAP J1745-5051. An isolated sub-set of the detected sources is used to estimate the FWHM of the PSF. The detected sources are cross-matched to the *Gaia* DR3 sources in the same field, and the resulting matches are used to refine the image world-coordinate system (WCS) slightly. We then

carry out forced PSF-fitting photometry on the locations of the *Gaia* sources in the field, adopting a Gaussian PSF with the FWHM estimated previously. We finally calibrate the photometry by cross-matching to the VHS catalogue and applying a zero-point that optimally matches our instrumental magnitudes to the VHS magnitudes. Our error budget thus includes contributions from noise in the images, from blending between sources and from the global calibration.

Figures 3 and 4 provide diagnostic plots that illustrate the quality of these fits for the J -band and one K_s -band image. It should be clear from these figures that the deblending process is difficult. The neighbour is clearly brighter than ASKAP J1745-5051 in the near-IR, and the 2-D brightness distribution shows only a *slight* elongation towards the target position (especially in the K_s band).

As a check on the systematics associated with this PSF-fitting procedure, we repeated the entire process, but this time assuming a Moffat PSF. There are then two PSF shape parameters – α and β . As before, these were estimated empirically from isolated sources in the field. Table 1 also lists these Moffat-PSF-based near-IR brightness estimates for ASKAP J1745-5051, which differ by 0.2 mag - 0.6 mag from those based on the Gaussian PSF. As expected, the Moffat-PSF-based estimates are systematically fainter, because this PSF has broader

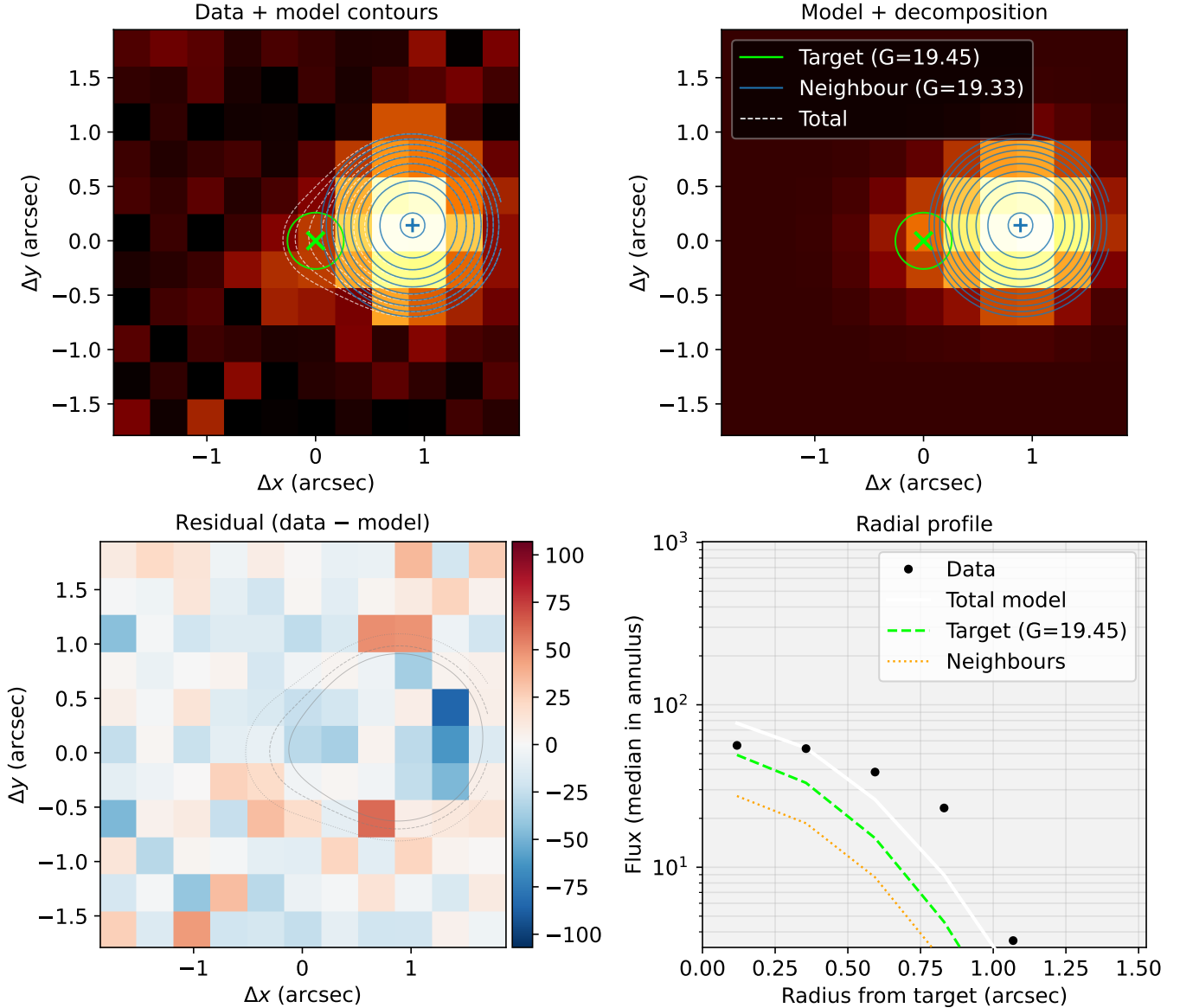


FIG. 3.— PSF fitting of the ESO-VISTA/VIRCAM K_s band with two Gaussian components. **Top left:** isocontours of model composite is shown with the dashed curve. The fitted position (and contours) for ASKAP J1745-5051 and the neighbour star are shown with an encircled \times and $+$ symbols in yellow and blue respectively. **Top right:** same as before but with no model overlaid. **Bottom left:** residual image after extracting the model. **Bottom right:** median flux of the en each annulus as a function of radius for the data, total model and each individual fit are shown with black dots, white solid line, green dashed line and dotted line respectively.

wings. As a result, a larger proportion of the flux at the position of ASKAP J1745-5051 is attributed to the neighbour. However, both Gaussian- and Moffat-PSF-fitting approaches produce magnitude estimates with *internal* uncertainties of 0.1 mag - 0.2 mag, suggesting that – regardless of the measurement approach – ASKAP J1745-5051 is at least marginally detected in these images. We will adopt the magnitude estimates obtained with the Gaussian PSF as our default. However, we will discuss the implications of these systematic uncertainties – including the possibility that the detections are false positives – in Section 4.

3. SED FITTING

In order to determine the physical properties of the ASKAP J1745-5051 binary system, we have carried out a simple 2-component model fit to the SED. The two components we consider are the WD primary and the low-mass secondary. We do not include any contribution from the accretion flow itself, such as an accretion disk or magnetic accretion curtains. The rationale for and implications of this choice are discussed in Section 4.2.

We use (Koester 2010) synthetic DA WD spectra to model the flux produced by compact primary in ASKAP

ESO-VISTA/VIRCAM/J | DATE-OBS=2014-07-28T03:16:16.7303

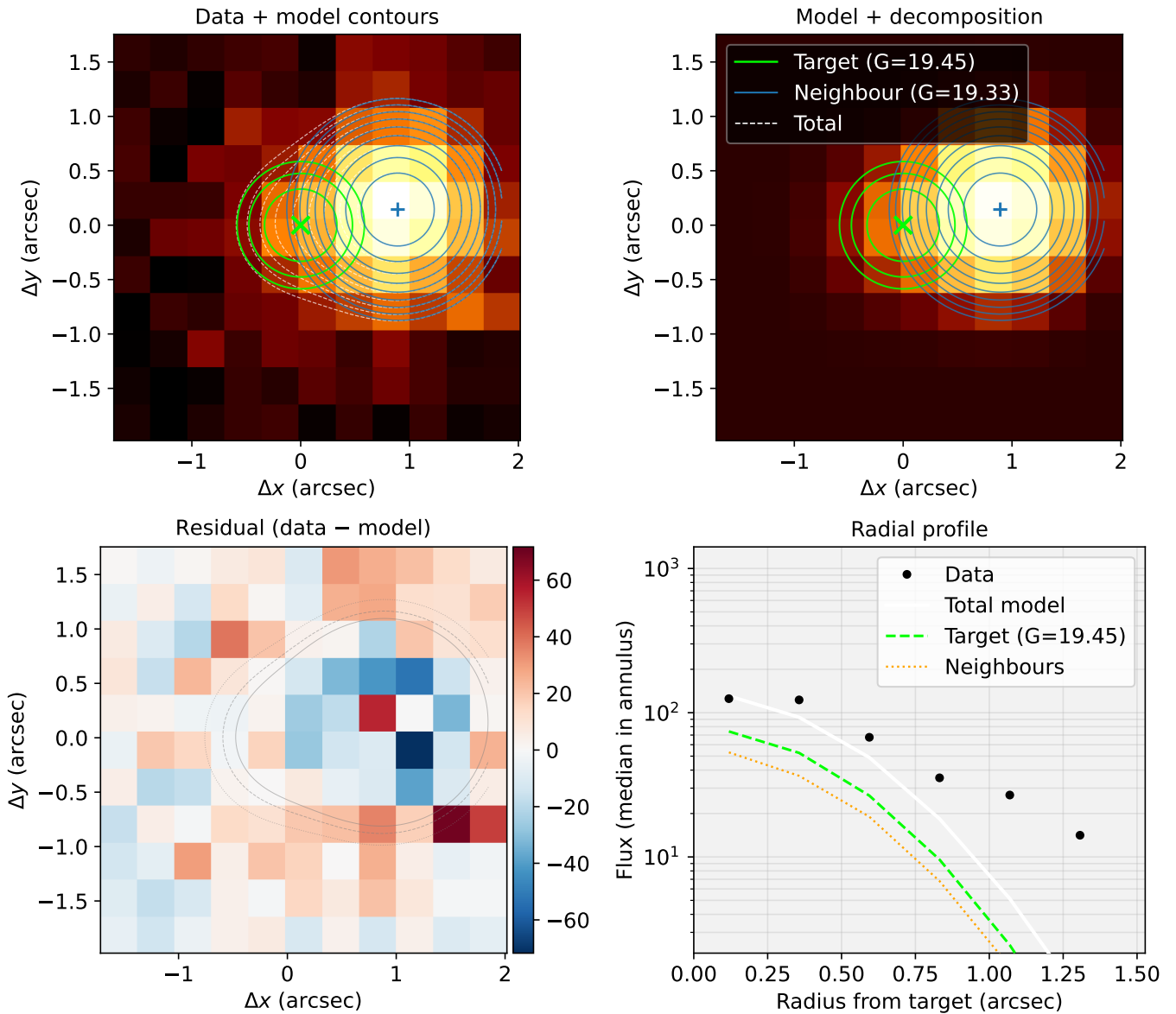


FIG. 4.— Same as Figure 3 but for ESO-VISTA/VIRCAM *J* band

J1745-5051. We adopt a mass of $M_{WD} \simeq 0.8 M_{\odot}$ for this component, roughly the average mass of WDs in CVs (e.g. Knigge et al. 2008; Littlefair et al. 2008; Savoury et al. 2011; Pala et al. 2020). The corresponding WD radius ($R_{WD} \simeq 7 \times 10^8$ cm) and surface gravity ($\log g \simeq 8.3$) are calculated from the WD cooling models of Bergeron et al. (1995, 2001). These values are actually slightly temperature-dependent, and we account for this in our fits.

Since the orbital period of ASKAP J1745-5051 is spectroscopically confirmed – $P_{orb} = 1.368 \pm 0.053$ hr = 82.1 ± 3.2 min – the secondary can be placed almost uniquely on the semi-empirical CV donor sequence (Knigge 2006; Knigge et al. 2011, hereafter KBP11). The placement is not quite unique, since this P_{orb} is very close to the minimum in the CV orbital period distribution, $P_{min} =$

82.4 ± 0.7 min (Gänsicke et al. 2009).

The period minimum exists because the direction of orbital period evolution depends only on the mass-radius index (ζ) of the donor. The critical point, where the direction reverses, corresponds to $\zeta \simeq 1/3$. A CV with a roughly main-sequence donor ($\zeta \simeq 1$) initially evolves from long to short orbital periods. However, the mass-losing donor must eventually reach the Hydrogen-burning limit and become a brown dwarf (e.g. Hernández Santisteban et al. 2016). Such sub-stellar objects are characterized by $\zeta \simeq 0$. Somewhere along the line therefore – it turns out very close to the stellar/sub-stellar transition – the direction of period evolution must turn around. CVs that have already evolved beyond P_{min} are expected to harbour sub-stellar donors and are often referred to as “post-period-minimum” systems or,

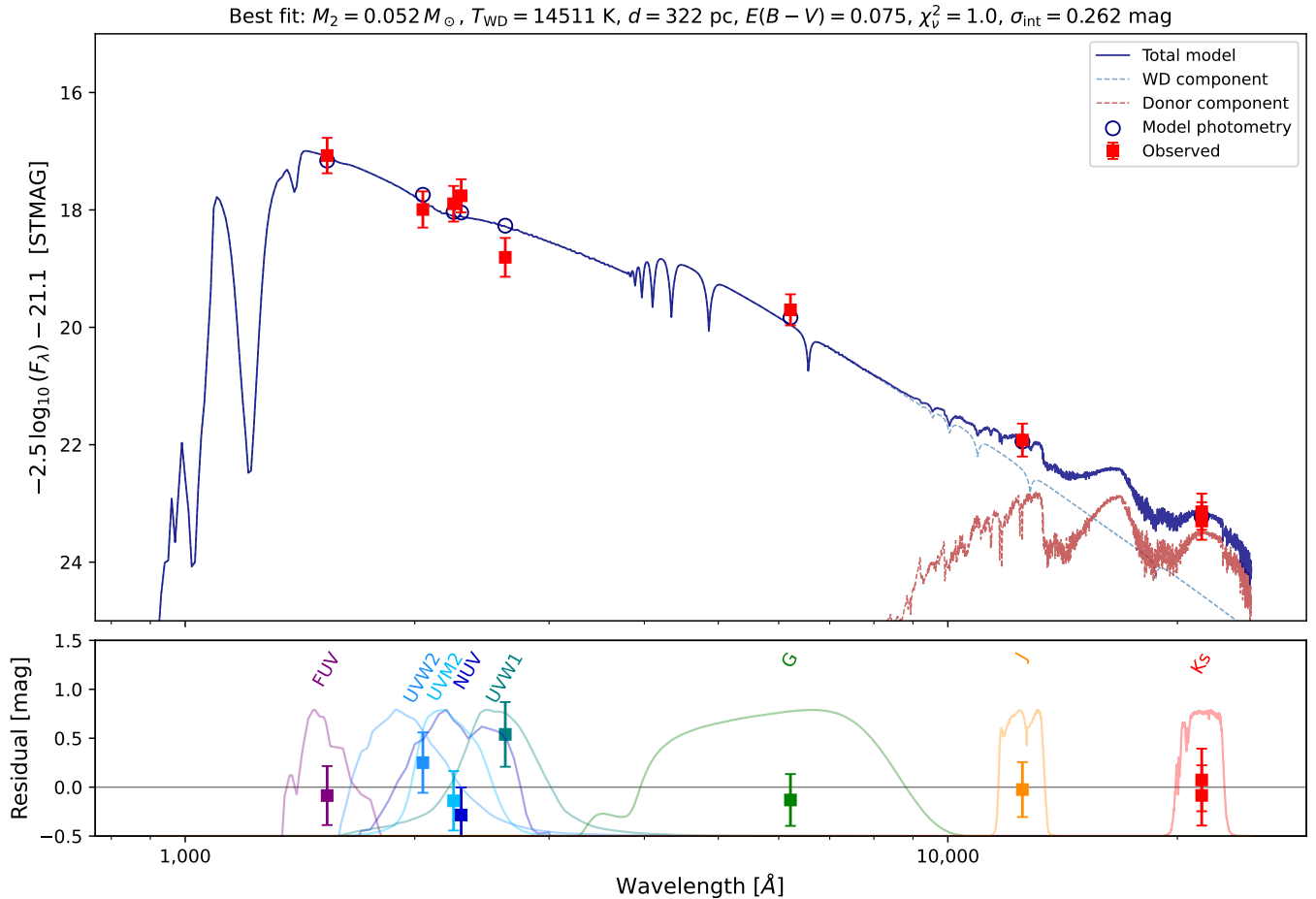


FIG. 5.— Spectral energy distribution of ASKAP J1745-5051 constructed using the PSF photometry derived in this work. The observed fluxes are shown as red squares. The SED is modelled with a DA white dwarf atmosphere and a late-type stellar companion atmosphere, shown by the purple and red dashed curves, respectively. The resulting composite model is shown by the purple solid curve, while the open circles indicate the corresponding synthetic photometry. The transmission function of each band is shown in the bottom panel, together with the fit residuals.

more casually, “period bouncers”.

ASKAP J1745-5051 orbital period is such that it could either be a pre- or a post-period-minimum system. Taking a $\simeq 2\sigma$ interval around P_{orb} , the KBP11 “optimal” donor sequence suggests that the allowed range of secondary masses is $0.04 \lesssim M_2/M_\odot \lesssim 0.09$. The existence of the donor sequence is a direct consequence of the fact that CVs are semi-detached binaries, and since ASKAP J1745-5051 is a confirmed CV, its donor *must* lie close to this sequence. We therefore constrain the component representing the secondary in our SED fit to lie on the KBP11 optimal sequence. For any given M_2 , this fixes R_2 (and hence $\log g_2$), but also the donor temperature, T_2 .

Since our SED fit extends from the far-UV to the near-IR, we have to account for reddening and extinction towards the source. In our SED fits, we model the effects of reddening via the Fitzpatrick (1999) extinction curve with $R_V = 3.1$. The maximum line-of-sight extinction is $A_V \simeq 0.6$ (Schlafly & Finkbeiner 2011), corresponding to $E(B - V) \simeq 0.19$ for our adopted $R_V = 3.1$.

With these assumptions, our SED fit has only four free parameters: (i) the temperature of the WD (T_{WD} ;

(ii) the mass of the donor (M_2); (iii) the reddening/extinction towards the source ($E(B - V)$); (iv) the distance towards the source (d). Given any combination of these parameters, we first calculate and sum the spectra of the two model component, apply the appropriate reddening and extinction, shift the model to the correct distance and then carry out synthetic photometry in the relevant filters.

We estimate the optimal model parameters – and their errors – by carrying out a Markov-Chain Monte Carlo (MCMC) fit with *dynesty*⁴ (Speagle 2020). In doing so, we adopt the following simple and conservative uniform priors:

- (i) $3.9 \leq \log(T_{WD} [\text{K}]) \leq 4.7$
- (ii) $0.04 \leq M_2/M_\odot \leq 0.1$
- (iii) $0 \leq E(B - V) \leq 0.3$
- (iv) $1.0 \leq \log(d [\text{pc}]) \leq 3.7$.

The best fit achieved by this simple model is shown in Figure 5 and the associated corner plot in Figure 6. The fit is qualitatively and visually reasonable, but we have

⁴ <https://zenodo.org/records/17268284>

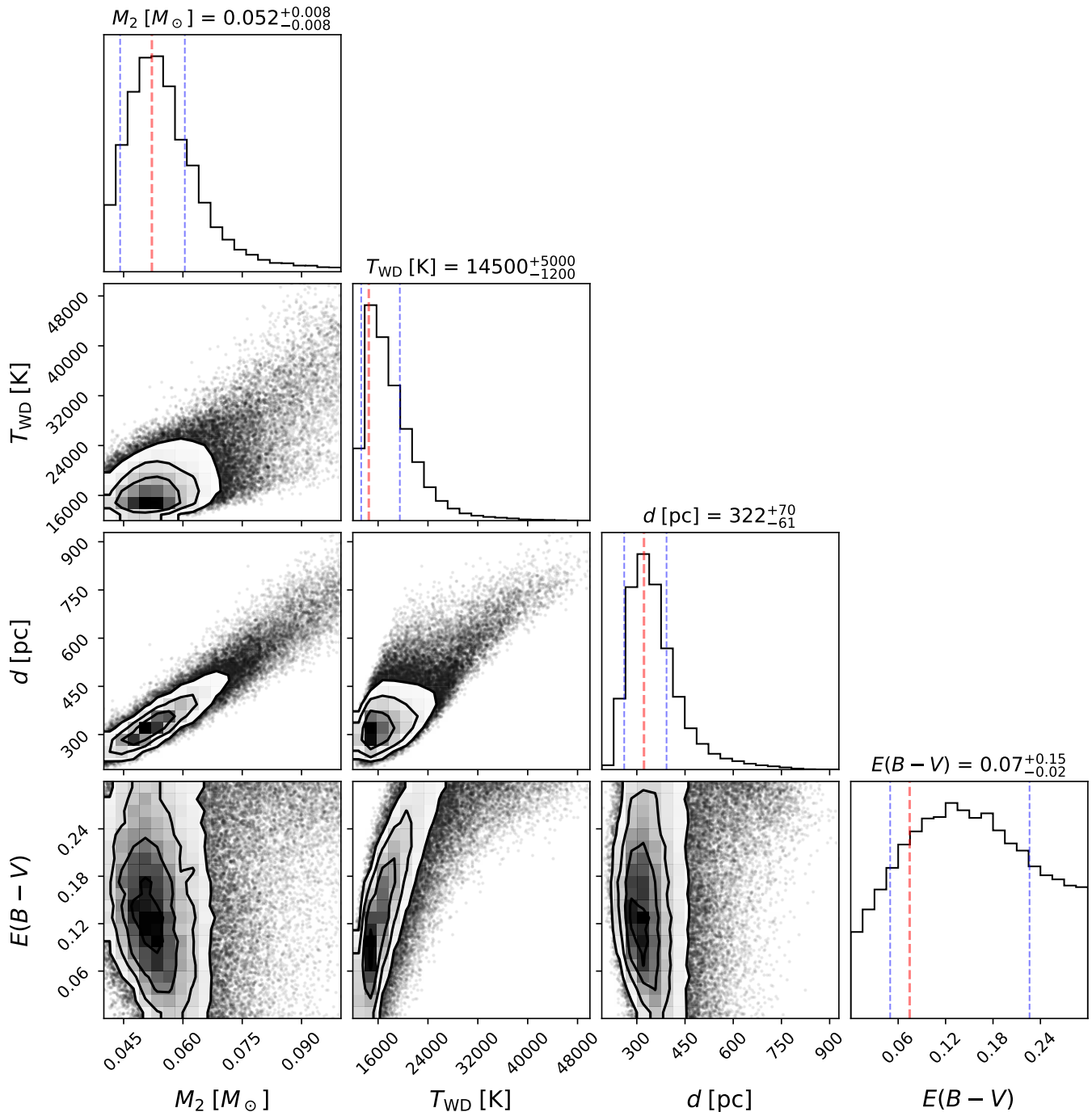


FIG. 6.— Posterior distributions of the ASKAP J1745-5051 system parameters inferred from the SED modelling presented in Figure 5. We adopted a WD mass of $M_{WD} = 0.8$ with radius $R_{WD} \simeq 7 \times 10^8$ cm and surface gravity $\log g \simeq 8.3$. The corner plot shows all fitted parameters except for the intrinsic scatter term, σ_{int} , which was added in quadrature to the uncertainties of all photometric measurements.

allowed for an intrinsic dispersion of $\sigma_{int} = 0.262$ to also make it statistically acceptable. This dispersion is added in quadrature to the observational error on each point ($\sigma_{obs,i}$), i.e. $\sigma_{total,i}^2 = \sigma_{obs,i}^2 + \sigma_{int}^2$. The value of σ_{int} is set by requiring that a statistically acceptable fit should achieve $\chi^2_\nu \simeq 1$. Without the intrinsic dispersion term, our best-fitting model achieves $\chi^2_\nu = 3.65$. Note that allowing for intrinsic dispersion term is conservative, in the sense that it increases the errors on the fit parameters. Of course, it is nevertheless important to ask whether

the required level of intrinsic scatter is reasonable, and we will return to this point below.

Overall, the best-fitting model does a reasonable job of reproducing the observed broad-band data. It suggests that a 15,000 K WD dominates the SED from the far-UV band through the optical region. The donor only begins to contribute significantly in the J band, before taking over in the K_s band. The best-fit mass of the donor puts it firmly in the sub-stellar regime.

The model parameters are all fairly well constrained by the data, although there are some degeneracies. All of

these can be understood, however. For example, the WD temperature is highly correlated with $E(B - V)$, since an increase in T_{WD} makes the model bluer, which can be counteracted by also increasing the reddening. Similarly, the distance preferred by the model is correlated with both donor mass and WD temperature, because increasing the distance makes both the WD and secondary model components fainter. The only way to counteract this WD [donor] flux decrease in the model is to increase the WD temperature [donor mass].

4. DISCUSSION

We have shown that a simple, physically motivated two-component model can provide a reasonable match to the far-UV through near-IR SED of ASKAP J1745-5051. The two components correspond to the accreting WD and its low-mass companion, with properties constrained by the mCV nature of this LPT. In particular, our model requires the donor mass, radius and temperature to fall on the CV donor sequence (Knigge 2006, KBP11). The best-fit parameters – $T_{WD} \simeq 14,500$ K, $M_2 \simeq 0.05 M_\odot$ (corresponding to $T_2 \simeq 1800$ K), $d \simeq 300$ pc and $E(B - V) \simeq 0.075$ – are all quite reasonable compared to other period-bounce CVs. That said, several aspects of this model merit additional comments.

4.1. *Is the model good enough? The need for intrinsic dispersion*

As noted in Section 3, we need to add an intrinsic dispersion of $\sigma_{int} \simeq 0.26$ mag (in quadrature) to the observational uncertainties in order for the model to achieve $\chi^2_\nu = 1$. Without any intrinsic dispersion, the best fitting model achieves $\chi^2_\nu = 3.65$. For a fit with $\nu = 5$ degrees of freedom (9 data points; 4 free parameters), this corresponds to a p-value of $p \simeq 0.003$. This p-value is the probability of finding a χ^2_ν as large as this if both the model and the errors are correct. Formally, this amounts to a 3σ rejection of the model. The *minimum* intrinsic dispersion needed – which we define as that required to reach $p \simeq 0.05$ – is $\sigma_{int,min} = 0.13$. Importantly, all of these fits – from $\sigma_{int} = 0$ mag to $\sigma_{int} = 0.26$ mag – produce almost identical best-fit parameters. What σ_{int} does affect is the size of the inferred parameter uncertainties. As pointed out in Section 3, allowing for intrinsic dispersion is conservative, in that it *increases* the parameter uncertainties.

In our view, the requirement for this level of intrinsic dispersion is not too concerning, either statistically or physically. Statistically, $\sigma_{int,min}$ is comparable to (or even smaller than) most of the observational errors in Table 1. These errors are inevitably uncertain themselves, e.g. due to blending (which definitely affects the NIR and might affect the NUV). Physically, there are at least two plausible explanations for the fit residuals that would not fundamentally alter our conclusions. First, the source may exhibit variability that manifests as intrinsic dispersion in the fit. In WD-dominated polars, a hot spot associated with the polar cap on the WD surface is one obvious way to generate variability on the orbital period (e.g. Gänsicke et al. 1995). The amplitude of such variations can exceed a factor of two in the far-UV band, more than sufficient to account for the observed fit residuals (but not so large that the fit would be qualitatively affected). Another form of variability is short-time-scale

stochastic “flickering”. This is more commonly associated with disk-accreting systems (Scaringi 2014), but is also seen in diskless polars (Ikiewicz et al. 2022). Second, since the WD is magnetic, its spectrum may exhibit significant cyclotron humps (Cropper 1990; Ferrario et al. 2015). These are not included in our model. The optical spectrum reported by Rose et al. (2026) does not reveal strong cyclotron features, but they could be more prominent in the ultraviolet (e.g. Gänsicke et al. 2001) or nIR (e.g. Campbell & Harrison 2007) depending on the WD surface magnetic field strength. These features could thus produce localized residuals without changing the overall character of the fit.

4.2. *Is the model too simple? The potential impact of missing model components*

A more significant concern is whether our model is too simple. In particular, it does not include any component associated with the accretion flow, assuming instead that the WD dominates everywhere shortward of the near-IR. In order to test the potential impact of this assumption, we have carried out two types additional fits. In the first, we allow for an extra blackbody (BB) component described by temperature T_{BB} and radius R_{BB} . In the second, we allow for an extra optically thick, truncated accretion disk. This disk is described as an area-weighted sum of blackbodies between inner radius R_{inner} and outer radius $R_{disk} = 30 R_{WD}$. The outer disk radius corresponds to the expected tidal radius for a system with $P_{orb} \simeq 1.3$ hr, $M_{WD} = 0.8 M_\odot$ and $M_2 \simeq 0.05 M_\odot$. For simplicity, we fix the inclination at $i = 60^\circ$. The free parameters are then R_{inner} and the accretion rate, \dot{M}_{acc} . Both of these are clearly just toy models for the accretion flow contribution. However, they provide a valuable check on the robustness of our simpler model.

Adding a single-temperature BB component to the model turns out to leave T_{WD} , M_2 , d and $E(B - V)$ almost unchanged. The optimal BB radius and temperature are $R_{BB} \simeq R_{WD}$ and $T_{BB} \simeq 7000$ K, making this component strongly sub-dominant everywhere. The fit quality also barely improves: for $\sigma_{int} = 0$, the raw χ^2 value associated with our best-fit simple model is $\chi^2 = 18.25$, while that associated with the more complex model is $\chi^2 = 17.64$. Unsurprisingly, the BB parameters are essentially unconstrained. Even if we force the BB component to dominate in the FUV – e.g. by setting $T_{BB} \simeq 50,000$ K and $R_{BB} \simeq 0.1 R_{WD}$, the remaining fit parameters change only modestly: $T_{WD} \simeq 11,000$ K, $M_2 \simeq 0.05 M_\odot$, $d \simeq 250$ pc and $E(B - V) \simeq 0.09$. Similarly, if we add a BB disk component to the model, the fit chooses to make this component negligible by driving \dot{M}_{acc} towards zero.

The only way to significantly alter the basic model parameters is to *force* the third component to dominate much of the SED, even at the cost of a worse fit. In such models, the distance is typically much larger, and the WD and donor parameters become poorly constrained. Most of these models are not physically plausible. For example, some require a very hot WD (to dominate in the far-UV despite a larger implied distance), while others simultaneously require a large distance and negligible reddening. However, with only 9 data points – and 6 parameters for these more complex models – we are clearly

in the data-poor regime. In order to determine the WD and donor properties definitively, additional observations – ideally far-UV and/or near-IR spectroscopy – will be required.

4.3. *The impact of systematic uncertainties affecting the near-IR brightness estimates*

As discussed in Section 2, our PSF-fitting near-IR brightness estimates are subject to considerable systematic errors. Depending on whether the PSF is modelled as a Gaussian or a Moffat profile, the inferred magnitudes can differ by up to 0.6 mag. Moreover, since the neighbouring star is significantly brighter than ASKAP J1745-5051 in the near-IR, even the significance of the detection itself may be questioned. However, treating the near-IR measurements as upper limits would simply tend to push the corresponding M_2 estimate even lower. In fact, this is exactly what happens when we repeat the fit after replacing the Gaussian-PSF near-IR brightness estimates with the fainter Moffat-PSF ones. This change moves the estimate of M_2 slightly downwards – from $0.052 M_\odot$ to $0.049 M_\odot$ – but otherwise leaves the fit largely unchanged. Our conclusions are therefore robust to these uncertainties.

4.4. *The WD temperature and implied accretion rate*

The WDs in CVs are thought to be accretion-heated (Townsley & Bildsten 2003). Thus T_{WD} can be used as a proxy for the accretion rate onto the WD, averaged over $10^3 - 10^5$ years and depending somewhat on the time since the most recent nova eruption of the system (Townsley & Gänsicke 2009). A WD temperature of 14,500 K corresponds to $\dot{M}_{acc} \simeq 8 \times 10^{-11} M_\odot \text{ yr}^{-1}$. By comparison, the best-fit location on the CV donor sequence – $M_2 \simeq 0.05 M_\odot$ – corresponds to a mass-transfer rate of $\dot{M}_{acc} \simeq 3 \times 10^{-11} M_\odot \text{ yr}^{-1}$ and a WD temperature of $T_{WD} \simeq 11,200$ K. Allowing for both observational errors and theoretical uncertainties, we consider these values to be consistent.⁵

Since ASKAP J1745-5051 most likely belongs to the polar class of mCVs, one theoretical uncertainty deserves special mention. KPB11’s optimal donor and CV evolution sequence allows for angular momentum loss (AML) in excess of that expected from gravitational radiation alone. The need for this is well established in non-magnetic CVs. However, there is reasonable evidence that polar-type mCVs, in which the WD magnetic field is strong enough to prevent the formation of an accretion disk, may *not* require enhanced AML (Townsley & Gänsicke 2009). In these systems, WD temperatures tend to be systematically lower – by perhaps a few thousand degrees – than in non-magnetic CVs.

4.5. *Evolutionary implications: space density and hidden LPTs among mCVs*

The closest confirmed polar-type mCV is AM Her at $d \simeq 88$ pc (e.g. Pala et al. 2020). The ratio of the space densities of “normal” polars and systems like ASKAP

J1745-5051 is therefore roughly $(322/88)^3 \simeq 60$. However, this estimate neglects that the detection of LPTs requires the observer to lie within the narrow radio beam. Based on Supplementary Table 1 in Rose et al. (2026), we estimate that the typical orbital phase width of the radio pulses in ASKAP J1745-5051 is $\Delta\phi \simeq 0.07$, corresponding to a beam half-opening angle of $\rho \simeq 25^\circ$. Let us assume that the beam is associated with a dipolar magnetic field whose axis is inclined by an angle α to the WD spin axis. The so-called “beaming fraction” – the fraction of the sky the beam sweeps out – is then $f_{beam} = \sin\alpha \sin\rho$ (e.g. Lorimer & Kramer 2004). For $\rho \simeq 25^\circ$, $f_{beam} \simeq 0.423 \sin\alpha$. If the magnetic inclination is modest – e.g. $\alpha \lesssim 15^\circ$, the *intrinsic* space density of systems like ASKAP J1745-5051 could be an order of magnitude higher than implied by its distance. Thus the percentage of mCVs that *produce* pulsed radio emission could actually be quite high. In this scenario, the reason we do not observe most of them as LPTs is simply that we are not aligned with the radio beam.

5. SUMMARY

We have constructed and modelled the far-UV through near-IR SED of the recently discovered LPT and mCV ASKAP J1745-5051. We find that the SED can be reasonably described by a simple two component model: an accretion-heated WD and a low-mass donor that is constrained to lie on the standard CV evolution track. Based on this analysis, our main results are as follows.

- (i) The far-UV through optical flux can be explained by emission from the $\simeq 15,000$ K WD.
- (ii) A sub-stellar donor of mass $M_2 \simeq 0.05 M_\odot$ begins to contribute in the near-IR and dominates the K_s band. With such a small donor mass, the system is likely to already have evolved past the period minimum and is likely to be a “period bouncer”.
- (iii) Our SED fit suggests a distance towards ASKAP J1745-5051 of $d \simeq 320 \pm 70$ pc.
- (iv) The space density implied by this distance corresponds to $\simeq 2\%$ of the mCV space density, but the beaming fraction may well be small. If so, the true percentage of LPTs among mCV could be far larger.

ACKNOWLEDGMENTS

We are grateful to Kovi Rose, both for their helpful responses to our questions and for making most of their data and analysis scripts publicly available via github and zenodo. The code associated with this paper was created with Generative AI (mostly Anthropic’s Claude), but always with a human – in this case the lead author – in the loop. The analysis and interpretation also benefitted from discussions with Claude. Responsibility for the results – and for any errors – rests solely with the authors, of course. SS is supported by STFC grants ST/T000244/1 and ST/X001075/1. DDM is supported by INAF, AF2022 FANS and AF2024 PULSE-X projects. NCS acknowledge support from the Science and Technology Facilities Council (STFC) grant ST/X001121/1.

⁵ Factors contributing to these “theoretical uncertainties” are the assumed WD mass, the poorly constrained CV angular momentum loss rates and the unknown time since the last nova eruption.

REFERENCES

- Anumrapapudi, A., Kaplan, D. L., Rea, N., et al. 2025, MNRAS, 542, 1208, doi: [10.1093/mnras/staf1227](https://doi.org/10.1093/mnras/staf1227)
- Archibald, A. M., Stairs, I. H., Ransom, S. M., et al. 2009, Science, 324, 1411, doi: [10.1126/science.1172740](https://doi.org/10.1126/science.1172740)
- Babusiaux, C., Fabricius, C., Khanna, S., et al. 2023, A&A, 674, A32, doi: [10.1051/0004-6361/202243790](https://doi.org/10.1051/0004-6361/202243790)
- Barrett, P., Dieck, C., Beasley, A. J., Mason, P. A., & Singh, K. P. 2020, Advances in Space Research, 66, 1226, doi: [10.1016/j.asr.2020.04.007](https://doi.org/10.1016/j.asr.2020.04.007)
- Barrett, P. E., & Gurwell, M. A. 2025, arXiv e-prints, arXiv:2505.06468, doi: [10.48550/arXiv.2505.06468](https://doi.org/10.48550/arXiv.2505.06468)
- Bergeron, P., Leggett, S. K., & Ruiz, M. T. 2001, ApJS, 133, 413, doi: [10.1086/320356](https://doi.org/10.1086/320356)
- Bergeron, P., Wesemael, F., & Beauchamp, A. 1995, PASP, 107, 1047, doi: [10.1086/133661](https://doi.org/10.1086/133661)
- Bloot, S., Vedantham, H. K., Bassa, C. G., et al. 2025, A&A, 699, A341, doi: [10.1051/0004-6361/202555131](https://doi.org/10.1051/0004-6361/202555131)
- Buckley, D. A. H., Meintjes, P. J., Potter, S. B., Marsh, T. R., & Gänsicke, B. T. 2017, Nature Astronomy, 1, 0029, doi: [10.1038/s41550-016-0029](https://doi.org/10.1038/s41550-016-0029)
- Camisassa, M., Fuentes, J. R., Schreiber, M. R., et al. 2024, A&A, 691, L21, doi: [10.1051/0004-6361/202452539](https://doi.org/10.1051/0004-6361/202452539)
- Campbell, R., & Harrison, T. E. 2007, in American Astronomical Society Meeting Abstracts, Vol. 211, American Astronomical Society Meeting Abstracts, 15.14
- Castro Segura, N., Pelisoli, I., Gänsicke, B. T., et al. 2025, MNRAS, 543, 2116, doi: [10.1093/mnras/staf1511](https://doi.org/10.1093/mnras/staf1511)
- Castro-Tapia, M., Zhang, S., & Cumming, A. 2024, ApJ, 975, 63, doi: [10.3847/1538-4357/ad7a6a](https://doi.org/10.3847/1538-4357/ad7a6a)
- Cropper, M. 1990, Space Sci. Rev., 54, 195, doi: [10.1007/BF00177799](https://doi.org/10.1007/BF00177799)
- de Ruiter, I., Rajwade, K. M., Bassa, C. G., et al. 2025, Nature Astronomy, doi: [10.1038/s41550-025-02491-0](https://doi.org/10.1038/s41550-025-02491-0)
- du Plessis, L., Venter, C., Wadiasingh, Z., et al. 2022, MNRAS, 510, 2998, doi: [10.1093/mnras/stab3595](https://doi.org/10.1093/mnras/stab3595)
- Ferrario, L., de Martino, D., & Gänsicke, B. T. 2015, Space Sci. Rev., 191, 111, doi: [10.1007/s11214-015-0152-0](https://doi.org/10.1007/s11214-015-0152-0)
- Fitzpatrick, E. L. 1999, PASP, 111, 63, doi: [10.1086/316293](https://doi.org/10.1086/316293)
- Gaia Collaboration, Vallenari, A., Brown, A. G. A., et al. 2023, A&A, 674, A1, doi: [10.1051/0004-6361/202243940](https://doi.org/10.1051/0004-6361/202243940)
- Gänsicke, B. T., Beuermann, K., & de Martino, D. 1995, A&A, 303, 127
- Gänsicke, B. T., Schmidt, G. D., Jordan, S., & Szkody, P. 2001, ApJ, 555, 380, doi: [10.1086/321464](https://doi.org/10.1086/321464)
- Gänsicke, B. T., Dillon, M., Southworth, J., et al. 2009, MNRAS, 397, 2170, doi: [10.1111/j.1365-2966.2009.15126.x](https://doi.org/10.1111/j.1365-2966.2009.15126.x)
- Garnavich, P., Littlefield, C., Kafka, S., et al. 2019, ApJ, 872, 67, doi: [10.3847/1538-4357/aafb2c](https://doi.org/10.3847/1538-4357/aafb2c)
- Garnavich, P., Littlefield, C., Lyutikov, M., & Barkov, M. 2021, ApJ, 908, 195, doi: [10.3847/1538-4357/abd4db](https://doi.org/10.3847/1538-4357/abd4db)
- Geng, J.-J., Zhang, B., & Huang, Y.-F. 2016, ApJ, 831, L10, doi: [10.3847/2041-8205/831/1/L10](https://doi.org/10.3847/2041-8205/831/1/L10)
- Hernández Santisteban, J. V., Knigge, C., Littlefair, S. P., et al. 2016, Nature, 533, 366, doi: [10.1038/nature17952](https://doi.org/10.1038/nature17952)
- Hurley-Walker, N., McSweeney, S. J., Bahramian, A., et al. 2024, ApJ, 976, L21, doi: [10.3847/2041-8213/ad890e](https://doi.org/10.3847/2041-8213/ad890e)
- Ikiewicz, K., Scaringi, S., Littlefield, C., & Mason, P. A. 2022, MNRAS, 516, 5209, doi: [10.1093/mnras/stac2597](https://doi.org/10.1093/mnras/stac2597)
- Imbrogno, M., Veresvarska, M., Wang, Y. L., et al. 2026, arXiv e-prints, arXiv:2606.05842, doi: [10.48550/arXiv.2606.05842](https://doi.org/10.48550/arXiv.2606.05842)
- Katz, J. I. 2017, ApJ, 835, 150, doi: [10.3847/1538-4357/835/2/150](https://doi.org/10.3847/1538-4357/835/2/150)
- Knigge, C. 2006, MNRAS, 373, 484, doi: [10.1111/j.1365-2966.2006.11096.x](https://doi.org/10.1111/j.1365-2966.2006.11096.x)
- Knigge, C., Baraffe, I., & Patterson, J. 2011, ApJS, 194, 28, doi: [10.1088/0067-0049/194/2/28](https://doi.org/10.1088/0067-0049/194/2/28)
- Knigge, C., Dieball, A., Maíz Apellániz, J., et al. 2008, ApJ, 683, 1006, doi: [10.1086/589987](https://doi.org/10.1086/589987)
- Koester, D. 2010, Mem. Soc. Astron. Italiana, 81, 921
- Littlefair, S. P., Dhillon, V. S., Marsh, T. R., et al. 2008, MNRAS, 388, 1582, doi: [10.1111/j.1365-2966.2008.13539.x](https://doi.org/10.1111/j.1365-2966.2008.13539.x)
- Lorimer, D. R., & Kramer, M. 2004, Handbook of Pulsar Astronomy, Vol. 4 (Cambridge University Press)
- Marsh, T. R., Gänsicke, B. T., Hümmelich, S., et al. 2016, Nature, 537, 374, doi: [10.1038/nature18620](https://doi.org/10.1038/nature18620)
- McMahon, R. G., Banerji, M., Gonzalez, E., et al. 2013, The Messenger, 154, 35
- Onken, C. A., Wolf, C., Bessell, M. S., et al. 2019, PASA, 36, e033, doi: [10.1017/pasa.2019.27](https://doi.org/10.1017/pasa.2019.27)
- Pala, A. F., Gänsicke, B. T., Breedt, E., et al. 2020, MNRAS, 494, 3799, doi: [10.1093/mnras/staa764](https://doi.org/10.1093/mnras/staa764)
- Papitto, A., & de Martino, D. 2022, in Astrophysics and Space Science Library, Vol. 465, Astrophysics and Space Science Library, ed. S. Bhattacharyya, A. Papitto, & D. Bhattacharya, 157–200, doi: [10.1007/978-3-030-85198-9_6](https://doi.org/10.1007/978-3-030-85198-9_6)
- Pelisoli, I., Marsh, T. R., Parsons, S. G., et al. 2022, MNRAS, 516, 5052, doi: [10.1093/mnras/stac2391](https://doi.org/10.1093/mnras/stac2391)
- Pelisoli, I., Marsh, T. R., Buckley, D. A. H., et al. 2023, Nature Astronomy, 7, 931, doi: [10.1038/s41550-023-01995-x](https://doi.org/10.1038/s41550-023-01995-x)
- Pelisoli, I., Sahu, S., Lyutikov, M., et al. 2024, MNRAS, 527, 3826, doi: [10.1093/mnras/stad3442](https://doi.org/10.1093/mnras/stad3442)
- Pelisoli, I., Brown, A. J., Castro Segura, N., et al. 2025, MNRAS, 544, L76, doi: [10.1093/mnras/slaf101](https://doi.org/10.1093/mnras/slaf101)
- Potter, S. B., & Buckley, D. A. H. 2018, MNRAS, 481, 2384, doi: [10.1093/mnras/sty2407](https://doi.org/10.1093/mnras/sty2407)
- Rea, N., Hurley-Walker, N., & Caleb, M. 2026, Journal of High Energy Astrophysics, 52, 100566, doi: [10.1016/j.jheap.2026.100566](https://doi.org/10.1016/j.jheap.2026.100566)
- Rodríguez, A. C. 2025, A&A, 695, L8, doi: [10.1051/0004-6361/202553684](https://doi.org/10.1051/0004-6361/202553684)
- Rose, K., Pritchard, J., Murphy, T., et al. 2026, Nature Astronomy, doi: [10.1038/s41550-026-02882-x](https://doi.org/10.1038/s41550-026-02882-x)
- Savourey, C. D. J., Littlefair, S. P., Dhillon, V. S., et al. 2011, MNRAS, 415, 2025, doi: [10.1111/j.1365-2966.2011.18707.x](https://doi.org/10.1111/j.1365-2966.2011.18707.x)
- Scaringi, S. 2014, MNRAS, 438, 1233, doi: [10.1093/mnras/stt2270](https://doi.org/10.1093/mnras/stt2270)
- Schlafly, E. F., & Finkbeiner, D. P. 2011, ApJ, 737, 103, doi: [10.1088/0004-637X/737/2/103](https://doi.org/10.1088/0004-637X/737/2/103)
- Schreiber, M. R., Belloni, D., Gänsicke, B. T., Parsons, S. G., & Zorotovic, M. 2021, Nature Astronomy, 5, 648, doi: [10.1038/s41550-021-01346-8](https://doi.org/10.1038/s41550-021-01346-8)
- Speagle, J. S. 2020, MNRAS, 493, 3132, doi: [10.1093/mnras/staa278](https://doi.org/10.1093/mnras/staa278)
- Takata, J., Hu, C. P., Lin, L. C. C., et al. 2018, ApJ, 853, 106, doi: [10.3847/1538-4357/aaa23d](https://doi.org/10.3847/1538-4357/aaa23d)
- Townsley, D. M., & Bildsten, L. 2003, ApJ, 596, L227, doi: [10.1086/379535](https://doi.org/10.1086/379535)
- Townsley, D. M., & Gänsicke, B. T. 2009, ApJ, 693, 1007, doi: [10.1088/0004-637X/693/1/1007](https://doi.org/10.1088/0004-637X/693/1/1007)
- Warner, B. 1995, Cataclysmic variable stars, Vol. 28 (Cambridge University Press)
- Yang, Y.-P. 2026, ApJ, 997, 124, doi: [10.3847/1538-4357/ae2864](https://doi.org/10.3847/1538-4357/ae2864)

This paper was built using the Open Journal of Astrophysics L^AT_EX template. The OJA is a journal which

provides fast and easy peer review for new papers in the **astro-ph** section of the arXiv, making the reviewing process simpler for authors and referees alike. Learn more at <http://astro.theoj.org>.